ELSEVIER

The *Drosophila* fragile X-related gene regulates axoneme differentiation during spermatogenesis

Yong Q. Zhang,[a] Heinrich J.G. Matthies,[a] Joel Mancuso,[a] Hillary K. Andrews,[a] Elvin Woodruff III,[a] David Friedman,[b] and Kendal Broadie[a,*]

[a] *Department of Biological Sciences, Vanderbilt Kennedy Center for Research on Human Development, Vanderbilt University, Nashville, TN, 37235-1634, USA*
[b] *Proteomics and Mass Spectrometry Research Center, Vanderbilt University, Nashville, TN, 37235-1634, USA*

Abstract

Macroorchidism (i.e., enlarged testicles) and mental retardation are the two hallmark symptoms of Fragile X syndrome (FraX). The disease is caused by loss of fragile X mental retardation protein (FMRP), an RNA-binding translational regulator. We previously established a FraX model in *Drosophila*, showing that the fly FMRP homologue, dFXR, acts as a negative translational regulator of microtubule-associated Futsch to control stability of the microtubule cytoskeleton during nervous system development. Here, we investigate dFXR function in the testes. Male *dfxr* null mutants have the enlarged testes characteristic of the disease and are nearly sterile (>90% reduced male fecundity). dFXR protein is highly enriched in *Drosophila* testes, particularly in spermatogenic cells during the early stages of spermatogenesis. Cytological analyses reveal that spermatogenesis is arrested specifically in late-stage spermatid differentiation following individualization. Ultrastructurally, *dfxr* mutants lose specifically the central pair microtubules in the sperm tail axoneme. The frequency of central pair microtubule loss becomes progressively greater as spermatogenesis progresses, suggesting that dFXR regulates microtubule stability. Proteomic analyses reveal that chaperones Hsp60B-, Hsp68-, Hsp90-related protein TRAP1, and other proteins have altered expression in *dfxr* mutant testes. Taken together with our previous nervous system results, these data suggest a common model in which dFXR regulates microtubule stability in both synaptogenesis in the nervous system and spermatogenesis in the testes. The characterization of *dfxr* function in the testes paves the way to genetic screens for modifiers of *dfxr*-induced male sterility, as a means to efficiently dissect FMRP-mediated mechanisms.
© 2004 Elsevier Inc. All rights reserved.

Keywords: Fragile X syndrome; Fertility; Axoneme; Microtubule; RNA binding protein; Translational regulation; Proteomics

Introduction

Fragile X syndrome (FraX) is the most common form of inherited mental retardation, occurring in 1/4000 males and 1/8000 females (Jin and Warren, 2000). FraX is caused by transcriptional silencing of the fragile X mental retardation 1 (*fmr1*) gene, which encodes FMRP, an RNA-binding protein acting as a translational regulator (Brown et al., 2001; Darnell et al., 2001; Jin and Warren, 2000; Laggerbauer et al., 2001; Li et al., 2001; Schaeffer et al., 2001; Zhang et al., 2001). In addition to compromised cognitive ability, the

most prominent FraX symptom is macroorchidism (i.e., enlarged testicles in post-pubescent male patients), suggesting a significant testicular defect. Although FraX male patients are fertile, including patients with a *FMR1* intragenic deletion (Malter et al., 1997; Reyniers et al., 1993), offspring of FraX male patients have been rarely documented (Jacobs et al., 1980; Meijer et al., 1994). A putative spermatogenesis defect was first reported in FraX patients nearly three decades ago (Cantu et al., 1976). Later, Johannisson et al. (1987) reported that the early stages of germ cell differentiation during spermatogenesis were normal in human patients, but that significantly malformed spermatids and a reduction of normally differentiated spermatids were observed in later stages of spermatogenesis. The FMR1 knockout mice established by Bakker et al. (1994) also display prominent macroorchidism. However, the litter size of knockout mice is reportedly normal and initial light

---

microscope analyses suggested normal spermatogenesis (Bakker et al., 1994). Nevertheless, late-stage spermatogenesis defects can escape scrutiny at the light microscopic level using standard histological analyses of testicles (Vollrath et al., 2001), and sperm counts as low as 30% of normal are known to cause normal mouse litter sizes (Schurmann et al., 2002). Therefore, a role for FMRP in testicular development and/or spermatogenesis has remained unsettled.

In mammals, there are three closely related FMRP family members: FMRP, FXR1P, and FXR2P. All three proteins are widely expressed, but particularly enriched in brain and testes (Bachner et al., 1993; Devys et al., 1993; Hinds et al., 1993; Huot et al., 2001). Comparative antibody staining of human testes samples has shown that the three proteins express differentially in fetal and adult testes (Tamanini et al., 1997); FMRP is highly expressed in spermatogonia, progenitors of spermotogenic cells, but not in mature germ cells or somatic Sertoli cells (Bachner et al., 1993; Devys et al., 1993; Hinds et al., 1993). FXR1P is also expressed in spermatogonia but predominantly in maturing spermatogenic cells, and FXR2P is present in all the cells throughout the seminiferous tubules. More intriguingly, Huot et al. (2001) recently showed that FXR1P is specifically associated with the microtubule cytoskeleton in the sperm tail, using biochemical, immunohistochemical, and electron microscopic techniques. These differential expression patterns suggest that the three homologous proteins of the FMRP family might have different functions in spermatogenesis. The *Drosophila* genome contains a single, well-conserved fragile X-related (*dfxr*) gene (Wan et al., 2000; Zhang et al., 2001), predicted to be ancestral to the three gene family members in mammals. Thus, *dfxr* is presumed to mediate the conserved functions of all three genes in the testes, simplifying the genetic analyses of their function in spermatogenesis. The spermatogenesis process is highly conserved between mammals and flies (Johannes et al., 2000), and *Drosophila* has provided an attractive model system for the study of spermatogenesis and its genetic controls (for reviews, see Fuller, 1993; Lindsley and Tokuyasu, 1980).

Previously, we established a *Drosophila* FraX model focusing on the nervous system aspects of the disease. In the nervous system, we showed that dFXR acts as a translational repressor of the MAP1 homologue Futsch to regulate synaptic development and function via a microtubule-based mechanism (Zhang et al., 2001). In the process of characterizing *dfxr* neurological functions, we observed that *dfxr* null mutants cannot be maintained as a stock with routine husbandry. Brooding tests demonstrated that male *dfxr* mutants are nearly sterile with fecundity reduced >90% compared to controls. Consistent with mammals, we show that dFXR is highly enriched in the testes during early stages of spermatogenesis before spermatid individualization, and that *dfxr* mutants show the enlarged testes characteristic of the disease. Unlike most other male-sterile mutants which display early-occurring and/or widespread spermatogenesis defects (for review, see Fuller, 1993), *dfxr*

mutants exhibit a highly specific, late-stage spermatogenesis arrest following spermatid individualization, resulting in individualized immotile sperm. Ultrastructural analyses reveal a progressive loss of the central pair of microtubules in the sperm tail flagellum, while the outer microtubule doublets remain intact, providing an explanation for sperm immobility and infertility. Comparative studies presented here in *fmr1* knockout mice for the first time also show late-stage spermatid defects suggesting an evolutionarily conserved mechanism. Newly available two-dimensional differential gel electrophoresis (2D DIGE) proteomics technology provides powerful quantitative comparisons of protein abundance changes with statistical confidence, but without the limitations normally associated with conventional 2D gel proteomic analysis (i.e., gel-to-gel variation, poor quantification. Alban et al., 2003; Friedman et al., 2004). When applied to the *dfxr* mutant testes, 2D DIGE revealed an intriguingly few protein groups with altered expression profiles in the absence of the dFXR translational regulator. Most interestingly, the chaperone proteins Hsp60B-, Hsp68-, and Hsp90-related protein TRAP1 display altered expression: Hsp60B and Hsp90 are required for spermatogenesis, and Hsp90 has been directly implicated in the regulation of microtubule dynamics (Timakov and Zhang, 2000; Yue et al., 1999). Taken together with our previous studies in the nervous system (Zhang et al., 2001), these data suggest a unifying mechanism in which *dfxr* regulates microtubule stability in both synaptogenesis and spermatogenesis.

Materials and methods

Drosophila stocks

All *Drosophila* stocks were raised at 25°C on standard cornmeal agar media. The wild-type strain was Oregon R (OR). Different *dfxr* mutant alleles were obtained from independent mutageneses in multiple laboratories. *dfxr*[50M], *dfxr*[83M], and *dfmr*[3] (also called *dfmr1*[3]: *dfxr* and *dfmr1* are synonyms of the same gene; *dfxr* is used in this report) are *dfxr* intragenic deletion lines characterized as protein null alleles; *dfxr*[9N] is a precise excision of the original P element insertion EP(3)3517 with the endogenous *dfxr* gene intact (Fig. 1A; Dockendorff et al., 2002; Morales et al., 2002; Zhang et al., 2001). A recombinant *FRT82B, dfxr*[50M] chromosome was generated based on conventional techniques, with a second site mutation of the original *dfxr*[50M] chromosome fortuitously crossed off; homozygous *FRT82B, dfxr*[50M] mutant flies were viable and readily obtainable. We therefore use the *FRT82B* homozygous stock (Bloomington stock center) as a genetic control, and the *FRT82B, dfxr*[50M] as a representative *dfxr* null allele. As a second genetic control, we used the *dfmr*[3] mutant containing a transgene of the wild-type *dfxr* gene under its native promoter regulation (*dfmr*[3]; res, a kind gift of Tom Jongens;
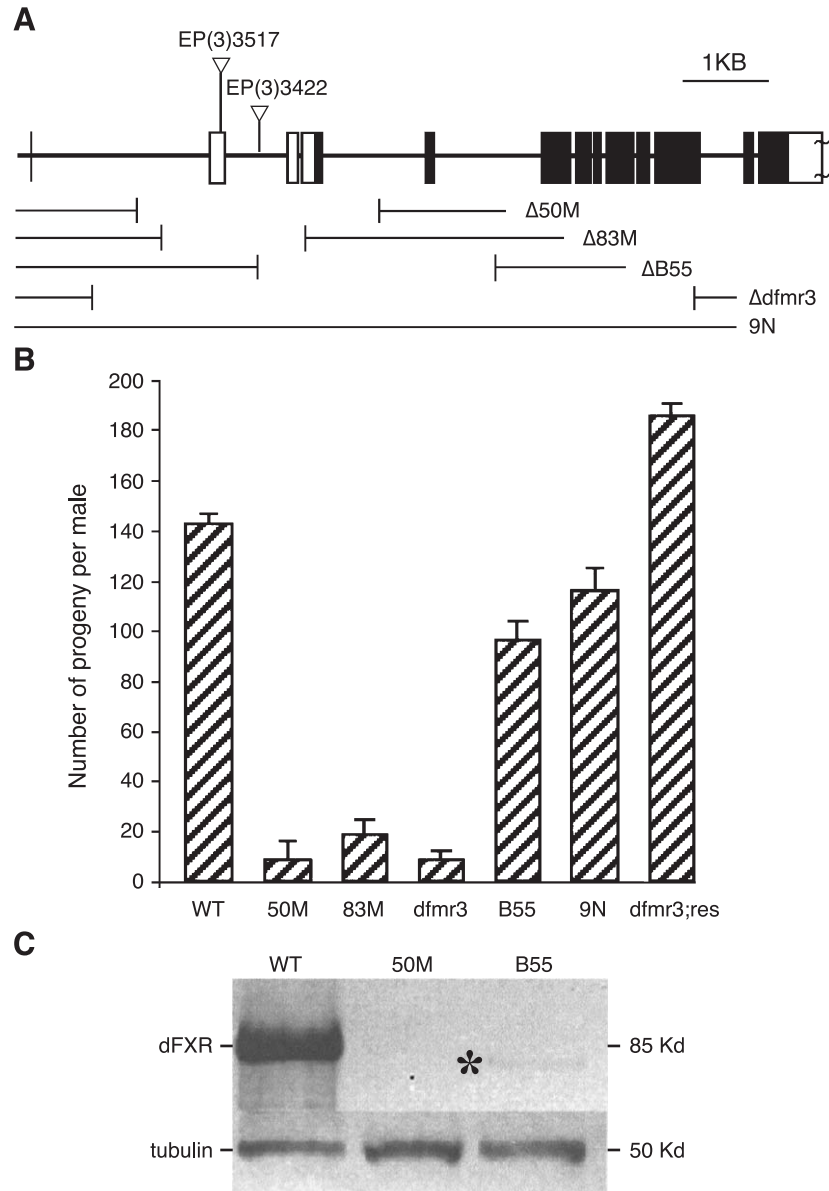
Fig. 1. *dfxr* gene structure, molecular nature of mutant alleles, and male fertility defects. (A) *dfxr* gene structure and the molecular nature of the mutant alleles used in this study. Two P element insertions, EP(3)3517 and EP(3)3422, are in the 5′regulatory region of *dfxr*. Imprecise excision lines *dfxr*[50M], *dfxr*[83M], and precise excision line *dfxr*[9N] were previously described in Zhang et al., 2001; imprecise excision line *dfxr*[B55] and *dfmr3* were described in Inoue et al., 2002, and Dockendorff et al., 2002, respectively. *dfxr*[B55] is derived from EP(3)3422; all others from EP(3)3517. Open box denotes non-coding exon; black box coding region; lines between boxes introns. " ~ " in the 3′ end indicates the gene structure is cut short to fit the space. Scale bar: 1 kb. (B) Fertility quantification of the number of progeny produced per male from brooding tests of different *dfxr* mutant alleles and controls: WT represents wild-type strain Oregon-R. *dfmr3*; res indicates the presence of a single copy of the wild-type *dfxr* transgene in *dfmr3* mutant background. Error bars indicate standard error of the mean. (C) Anti-dFXR Western analyses of adult testes. Strong dFXR expression is observed in wild-type (WT) testes. All imprecise excision alleles display no detectable dFXR expression in testes (*dfxr*[50M] shown), except the *dfxr*[B55] allele with greatly reduced expression and a slightly reduced protein size shown by asterisk. Anti-tubulin is used as a loading control. Loading of *dfxr*[50M] and *dfxr*[B55] is twice that of wild type. Protein sizes are indicated on the right.

Dockendorff et al., 2002). Another independent allele, *dfxr*[B55], also reported as a protein null allele of *dfxr*, was a gift from Haruhiko Siomi (Inoue et al., 2002). A transgenic construct with the Don Juan protein fused to GFP (Don Juan-GFP, DJ-GFP) under the control of the endogenous DJ promoter was used to visualize late-stage spermatids after the individualization process is initiated (Santel et al., 1998). A stock carrying DJ-GFP on the X chromosome and *dfxr*[50M]

on the third chromosome was made following standard genetic techniques to better characterize the role of *dfxr* in spermatogenesis.

Fertility quantification

Male brooding tests were performed essentially as described in Regan and Fuller (1988). Individual males of

each genotype were mated to three wild-type OR virgin females and transferred after 9 days at 25°C to fresh vials. Progeny from the original vial and the first transfer vial were counted through the 18th day after each mating. At least 17 males from each genotype were tested. For female fertility tests, 25 virgins of mutant $dfxr^{50M}$ or wild-type OR were crossed with 25 OR males in laying pots. Eggs were collected for 10 h from agar plates with yeast paste every other day from days 1 to 7. Fertility was analyzed by quantifying hatched larvae after 36 h at 25°C.

Quantification of testes size and cytological analyses of spermatogenesis

Testes from staged animals, <12 h or 24–36 h after eclosion, were dissected as described in Kemphues et al. (1980). For quantification of testis size, the dissected testes were fixed in 4% paraformaldehyde for 30 min, rinsed with PBS twice, then mounted on slides with Vectashield. The largest measurement of testis diameter at the tip or around the middle of the testes was recorded and statistically analyzed. For cytological analyses of spermatogenesis, testis squashes were examined for spermatogenic cells of stages before, during, or shortly after meiosis with phase contrast microscopy. For examination of gross morphology of testes and differentiating spermatids, whole-mount-fixed testes were visualized under transmission light, Nomarski or fluorescence optics with a Zeiss Axiophot II microscope.

Western analyses, immunohistochemistry, and DNA dye staining

Western analyses were done essentially as described by Wan et al. (2000). For sample preparation, adult testes of control flies and *dfxr* mutants were dissected in PBS buffer and transferred to 35 μl PBST (PBS with addition of 0.3% Triton X-100) plus 2 μl 25 × proteinase inhibitor (Roche), ground to completion on ice and then added 45 μl 2× Laemmli protein loading buffer. The samples were then subjected to SDS-PAGE, transfer and immunochemical detection. The *dfxr* antibody was a kind gift from Gideon Dreyfuss (Wan et al., 2000), used at 1:1000. α-tubulin antibody (clone B-5-1-2) was from Sigma and used at 1:2000. For antibody/dye staining on whole-mount preparations, larval testes and adult testes were dissected intact in TB1 buffer (7 mM K_2HPO_4, 7 mM KH_2PO_4, 80 mM KCl, 16 mM NaCl, 5 mM $MgCl_2$, and 1% PEG6000). The samples were fixed in 4% paraformaldehyde in PBS for 40 min, blocked in PBST plus 1% BSA three times for 10 min each, and then processed either with histological dyes or for immunocytochemistry. For nuclear staining on whole-mount adult testes, samples were incubated in diamidino-phenylindole (DAPI, 33 ng/ml H_2O) for 5 min or in propidium iodide (PI, 1.25 μg/ml in PBS) for 20 min followed by washing with PBST (3 × 10 min). Testis squashes for antibody staining were done as follows. Testis

squashes on slides were fast frozen in liquid N_2, followed by removal of the coverslip with a razor blade. The squashes were first fixed in 100% ethanol for 5 min then fixed with 4% paraformaldehyde in PBS for 30 min, blocked with PBST-BSA three times each for 10 min, then processed for immunocytochemistry as described (Zhang et al., 2001). The following antibodies were used for immunostaining: monoclonal anti-*dfxr* (1:1000; Wan et al., 2000), anti-α-tubulin FITC conjugate (1:50; Sigma), and Texas red phalloidin for F-actin staining (1:200; Molecular Probes, Eugene, OR). Secondary fluorescence-conjugated anti-mouse was used for visualization (Molecular Probes). The processed samples were mounted with Vectashield and visualized with a Zeiss Axiophot microscope equipped with a standard UV epifluorescence source or a DAPI fluorescence-selective emission filter (blue, 461 nm); images were captured with a cooled CCD digital camera (SPOT; Diagnostic Instruments Inc.) and processed with Adobe Photoshop. Serial sections of antibody or dye-stained preparations were acquired on a Zeiss LSM 510 Meta laser-scanning microscope.

Electron microscopy

Ultrastructural analyses of *Drosophila* testes of wild-type and multiple mutant alleles were done using standard protocols. Briefly, testes of 1- to 3-day-old males were dissected in TB1 buffer and immediately fixed for 3 h in 2.5% glutaraldehyde in 0.1 M cacodylate buffer (CB1, pH 7.2; note, fixation in 2.5% glutaraldehyde in TB1 buffer did not work as well as in CB1 buffer to preserve microtubule structure). The samples were subsequently rinsed with CB1 buffer, postfixed in 1% OsO_4 for 1 h, stained en bloc with aqueous 2% solution of uranyl acetate for 30 min, dehydrated through an ethanol series, and transferred into Epon resin. Ultrathin sections (60–70 nm, silver-gray) were obtained using a Reichert Ultracut E microtome with a diamond knife. Sections were cut at the base where the testes coil. At this point, sections are likely to contain both coiling spermatid cysts near the seminal vesicles and early-stage spermatid cysts at the straight portion of the testes. Sections were examined on a Hitachi H-7100 TEM and captured by a Gatan digital camera. For quantification of axoneme phenotypes, at least five cysts, each contains 64 spermatids, from different sections of each genotype, were scored under high resolution for absence of central pair of microtubules; no detectable presence of central pair of microtubules is defined as missing. For the examination of spermatogenesis in *fmr1* knockout mice, testes including epididymis were dissected out and fixed in 2.5% glutaraldehyde in PBS overnight at 4°C and then processed with standard procedures, as above. Spermatogenesis in testes and epididymis were examined separately. FVB mice with clean-up background (backcrossed 11 times with blind and albino coat color bred off FVB) were used as control animals. *fmr1* knockout mice in the clean-up FVB back-

ground were assayed for FMRP's role in fertility and spermatogenesis. Both strains of mice were gifts of Frank Kooy via Bill Greenough.

Proteomic analyses

2D difference gel electrophoresis (DIGE) using a mixed sample internal standard, spot identification by mass spectrometry, and database searching were done largely according to Friedman et al. (2004). For each of three independent replicate experiments, 20 testes from freshly eclosed males (<12 h) of each genotype, genetic control w^{1118}; *FRT82B* and mutant animal w^{1118}; *FRT82B, dxfr*^{50M}, were ground to completion in 100 μl lysis buffer (7M urea, 2M thiourea, 4% CHAPS, 17 mM DTT), precipitated with methanol/chloroform and resuspended in 100 μl lysis/labeling buffer (7 M urea, 2 M thiourea, 4% CHAPS, 30 mM Tris, 5 mM magnesium acetate) before labeling with 200 pmol of either Cy3 (control) or Cy5 (mutant). In a similar fashion, 60 testes, 10 from each of the six samples (three controls and three mutants), were processed and labeled with 600 pmol Cy2 (6-mix) as internal control for the three different gels. The labeled samples were combined such that each pairwise Cy3/Cy5-labeled sample was mixed with an equal aliquot of the Cy2-labeled mixed sample; in total, 30 testes (10 testes of each labeled samples of control, mutants, and 6-mix) were loaded on one gel. The three sets of tripartite-labeled samples were separated by standard 2D gel electrophoresis using an IPGphor first-dimension isoelectric focusing unit and 24 cm 4–7 immobilized pH gradient (IPG) strips (Amersham Biosciences), followed by second-dimension 12% SDS-PAGE using an Ettan DALT 12 unit (Amersham Biosciences) according to the manufacturer's protocols. The Cy2 (mixed standard), Cy3 (control), and Cy5 (mutant) components of each gel were individually imaged using mutually exclusive excitation/emission wavelengths of 480/530 nm for Cy2, 520/590 nm for Cy3, and 620/680 nm for Cy5 using a 2D 2920 Master Imager (Amersham Biosciences). A Sypro Ruby post-stain (Molecular Probes) was used to ensure accurate protein excision, as the low stoichiometry of Cy dyes label only 1–3% of the total protein. DeCyder software (Amersham Biosciences) was used for simultaneous comparison of abundance changes across all three sample pairs with statistical confidence and without interference from gel-to-gel variation (Alban et al., 2003; Friedman et al., 2004). Control/mutant volume ratios for each protein were calculated relative to the internal standard present on every gel and were used to calculate average abundance changes and Student's *t* test *P* values for the variance of these ratios for each protein pair across all three independent gels. Proteins of interest were excised and digested in-gel with modified porcine trypsin protease (Promega). Matrix-assisted laser desorption/ionization, time-of-flight (MALDI-TOF) mass spectrometry was performed on a Voyager 4700 (Applied Biosystems). Ions specific for each sample were used to interrogate *Drosoph-*

ila sequences deposited in the SWISS-PROT and NCBI databases using the MASCOT (http://www.matrixscience.com) and ProFound (prowl.rockefeller.edu) database search algorithms, respectively. Ions and homology score using the two algorithms are available upon request. Preliminary run of the whole procedure showed infection of *dfxr* mutants with *Wolbachia*, but the infection was eradicated with an antibiotic treatment following standard protocols. The clean-up stock was confirmed by PCR and the proteomic approach.

Results

Drosophila Fragile X-related (dfxr) mutants display reduced fertility

Mutations in the *dfxr* gene have been made independently in multiple laboratories. In each case, the starting point was a P-element transposon insertion, EP(3)3517 or EP(3)3422, in the 5′ regulatory region of the *dfxr* gene (Fig. 1A). Nested intragenic deficiencies have been made by imprecise excision of the P-elements, four of which are employed here: *dfxr*^{50M} and *dfxr*^{83M} (Zhang et al., 2001), *dfxr*^{B55} (Inoue et al., 2002), and *dfmr*^{3} (Dockendorff et al., 2002) (Fig. 1A). As a control for genetic background, a precise excision (*dfxr*^{9N}) has been maintained from the same screen that generated *dfxr*^{50M} and *dfxr*^{83M} alleles (Zhang et al., 2001). Additionally, a transgene of the wild-type *dfxr* gene under endogenous regulatory control is used to assay rescue of mutant phenotypes in *dfmr*^{3} mutant background (Dockendorff et al., 2002).

Homozygous or hemizygous *dfxr* mutant alleles are fully viable but cannot be maintained as stocks using standard fly husbandry. Both male and female mutants display significantly reduced fecundity when crossed to the wild-type OR strain. When crossed to wild-type males, *dfxr* null females (*dfxr*^{50M}) produce only 21% of the progeny of control females (data not shown), indicating that *dfxr* females have compromised fertility. This report, however, focuses exclusively on the role of dFXR in male spermatogenesis. Brooding test of individual males of three different *dfxr* alleles, *dfxr*^{50M}, *dfxr*^{83M}, and *dfmr*^{3} (Fig. 1B), show that *dfxr* males have greatly compromised fertility with very few progeny (mean ± SD: 8 ± 8, 18 ± 6, 8 ± 3 per male, respectively; $N > 17$). The precise excision line *dfxr*^{9N} shows fertility comparable to the wild-type control (115 ± 9 compared to 142 ± 4 per male), and the fertility defect is fully rescued with one copy of the wild-type *dfxr* transgene (185 ± 5 per male; Fig. 1B). Taken together, these data demonstrate that a severe male fertility defect is caused specifically by the absence of dFXR.

Given these results, it was surprising that the recently reported null *dfxr* allele *dfxr*^{B55} (Inoue et al., 2002) displays only a small reduction in male fertility (Fig. 1B). In contrast to all other *dfxr* mutants, homozygous *dfxr*^{B55} mutants can

be easily maintained as a stock. Similarly, $dfxr^{B55}$ has no eclosion rhythm defect (Inoue et al., 2002), whereas other $dfxr$ null alleles display fully consistent behavioral phenotypes including eclosion rhythm defects (Dockendorff et al., 2002; Morales et al., 2002). These contradictions suggest that the $dfxr^{B55}$ allele might not represent the null $dfxr$ condition. To test this possibility, we performed immunochemical analyses on $dfxr^{B55}$ mutant testes. Western analyses on testes reveal that $dfxr^{B55}$ mutants do indeed have residual dFXR expression, estimated to be approximately 5% of the wild-type protein level in testes (Fig. 1C). The other $dfxr$ alleles show no detectable protein ($dfxr^{50M}$ shown, Fig. 1C). The slightly smaller size and reduced amount of the dFXR protein detected in the Western blot (Fig. 1C) are consistent with the molecular nature of the B55 deletion, which deletes largely introns and three small exons encoding the N-terminal 38 aa (Fig. 1A; the first two coding exons encode 34 aa, but the first in-frame start codon ATG after the deletion encodes Met 39). In addition, immunocytochemistry with a monoclonal dFXR antibody in the testes reveals reduced but obvious protein expression in the $dfxr^{B55}$ allele (Fig. 2E). Most interestingly, the dFXR-positive cells are present in a mosaic fashion among spermatogenic cells in the testes, suggesting that an important tissue-specific regulatory sequence is disrupted in $dfxr^{B55}$ (Fig. 1A). The fact that the truncated dFXR protein predicted from the B55 deletion is detected by Western blot and the mosaic dFXR expression in the testes, indicate that

the $dfxr^{B55}$ allele is a hypomorphic allele, rather than a protein null, in contrast to the published report (Inoue et al., 2002). The mosaic persistence of dFXR in the $dfxr^{B55}$ hypomorph allele explains the maintenance of male fertility and supports the conclusion that dFXR expression in only a subset of spermatogenic cells is sufficient to restore near-normal male fecundity.

dFXR is highly expressed in spermatocytes during spermatogenesis

Drosophila spermatogenesis follows a stereotyped process of cell division, growth, and differentiation beginning with spermatogonium differentiation from a population of germline cells. A spermatogonium, in turn, undergoes four rounds of mitotic cell divisions to become early spermatocytes, which grow into much larger, late-stage spermatocytes. The late-stage spermatocytes then go through meiosis to become haploid spermatids, followed by dramatic differentiation steps to transform into greatly elongated mature spermatozoa. As a first step towards understanding the requirement of dFXR in male fertility, we performed immunostaining on testes to chart dFXR expression relative to the stages of spermatogenesis.

Immunocytochemistry on whole-mount testes showed that dFXR is highly expressed in both larval and adult testes (Fig. 2). In both larval and adult testes, dFXR is expressed in spermatogonia at low/modest levels, and in
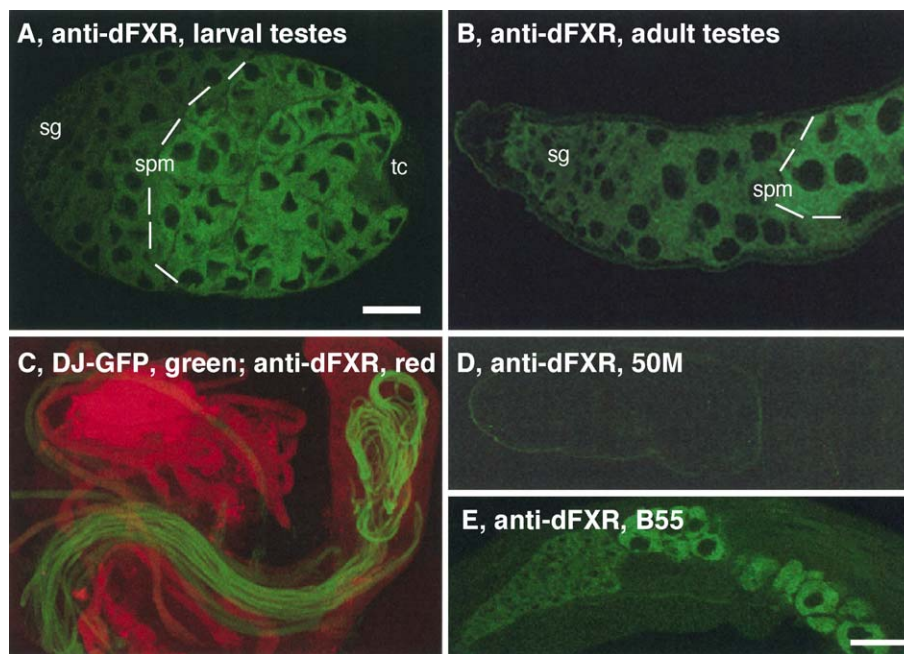
Fig. 2. dFXR protein is highly expressed in testes in the early stages of spermatogenesis before spermatid individualization. dFXR is highly expressed in both larval (A) and adult (B) testes. Sg: spermatogonia; spm, spermatocyte; tc, terminal cells. Dash lines indicate the border of spermatocytes expressing different levels of $dfxr$; weaker expression in early spermatocytes, stronger expression in late spermatocytes. Scale bar: 25 μm. (C) The dFXR-expressing spermatid bundles (in red) are not labeled with DJ-GFP (in green), demonstrating that dFXR is expressed in early, but not late, elongated spermatids. (D) $dfxr$ null alleles ($dfxr^{50M}$ shown) show no detectable dFXR expression in the testes. (E) In $dfxr^{B55}$, dFXR is expressed at reduced level in spermatocytes in a mosaic fashion. Note that the exposure time for D and E is longer than in B, as revealed by the higher background.

spermatocytes, especially later and larger spermatocytes, at highly enriched levels (Figs. 2A and 2B). In contrast, the expression of dFXR in the somatic terminal cells is undetectable or negligible. Relative to the high-level spermatocyte expression, dFXR is expressed at much lower levels in elongated spermatids (data not shown). dFXR is exclusively present in the soma of spermatogenic cells, and excluded from the nucleus, consistent with the previously reported sub-cellular pattern in the nervous system (Morales et al., 2002; Zhang et al., 2001).

Spermatid differentiation from the round haploid cell to the long-tailed mature spermatozoa lasts 4 days at 25°C in six recognizable stages: pre-elongation, elongation, transition, post-elongation, individualization, and coiling (Lindsley and Tokuyasu, 1980). To determine the specific stages of spermatid differentiation during which dFXR is expressed, we stained testes labeled with Don Juan-GFP (DJ-GFP), a specific label for late-stage elongated spermatids following initiation of the individualization process (Santel et al., 1998). As shown in Fig. 2C, the expression pattern of dFXR does not overlap with that of DJ-GFP, indicating that dFXR expression is restricted to the early stages of spermatid differentiation (stages 1–4) before individualization. Consistent with this conclusion, no dFXR expression is observed in mature spermatozoa stored at the base of testes or in the seminal vesicles (data not shown). As a control for the antibody specificity, no signal was observed in dfxr null mutants (Fig. 2D, dfxr^{50M} shown). As discussed above, dFXR is expressed in the spermatogenic cells in a mosaic fashion in the hypomorphic dfxr^{B55} allele (Fig. 2E). Taken together, these data show that dFXR is highly expressed in spermatocytes and modestly in the early stages of spermatid differentiation before individualization, a pattern which is similar to the composite expression profile of mammalian FMRP family (Tamanini et al., 1997).

dfxr mutants have enlarged testes and defective late-stage spermatogenesis

A diagnostic feature of Fragile X syndrome is prominently enlarged testes. Similarly, the mouse fmr1 knockout also exhibits enlarged testes (Bakker et al., 1994). This defect is reported to result from overproliferation of Sertoli cell during testicular development (Slegtenhorst-Eegdeman et al., 1998). In Drosophila, the dfxr null mutant testes are similarly grossly enlarged relative to controls (compare Figs. 3A and 3B). In quantified assays of young animals (<12 h post-eclosion), the diameter at the tip of testes was relatively comparable (130 ± 15 μm in controls versus 141 ± 15 μm in dfxr mutants with no significant difference ($P > 0.05$, $N > 14$; Fig. 3E)). In contrast, the diameter in the middle of testes was 230 ± 26 μm in mutants compared to 154 ± 22 μm in controls, a significant expansion ($P < 0.0001$, $N > 14$; Fig. 3E). This phenotype is 100% penetrant in newly eclosed flies (<12 h), but it abates with aging for reasons unknown (no

significant difference found in 3 days old flies). Other than this characteristic enlargement, the overall morphology of dfxr mutant testes appears normal. The length of testes showed no significant changes between controls and dfxr mutants (data not shown). The enlarged testes in dfxr mutants were also present in all null mutant alleles, and rescued with a single copy of the wild-type dfxr transgene (data not shown), demonstrating the specificity of the phenotype associated with dfxr mutation. It would be interesting to see if other sterile mutants have similar phenotypes.

The enlargement of dfxr mutant testes is limited to the basal two thirds of testes where the highly elongated spermatids are located (Figs. 3A and 3B). There are two possibilities for the enlargement, it could be due to the overproduction of spermatid bundles, a defect compatible with what can be inferred from a previous mammalian study (Slegtenhorst-Eegdeman et al., 1998), or it might result from misplacement of developmentally arrested spermatid bundles without any increase in proliferation. To address the mechanisms underlying the enlargement of mutant testes, the number of spermatid bundles was quantitatively assayed by DAPI staining of testes squashes (Figs. 3C and 3D). The results indicate no significant increase in the proliferation of spermatids in the dfxr mutant testes. In mutants, there is a mean of 38.55 ± 9.86 nuclei per testis, and in controls, 43.80 ± 7.94 nuclei per testis, showing no significant difference ($P > 0.2$, $N > 10$). In wild-type testes, the spermatid bundles are laid along the outer edge of testis lumen (Fig. 3A), whereas in the mutants, the spermatids filled the basal two-thirds testis lumen in an irregular fashion (Fig. 3B). These results suggest that the enlargement of testes in dfxr mutants results from the accumulation of misarranged spermatid bundles within the testis lumen, rather than from overproduction of spermatogenic cells. It appears that the mechanisms governing the enlargement of testes are different between fruitflies and mammals (also see below).

Phase contrast microscopy of testes squashes reveals no gross abnormalities in the mutants; spermatocytes divide and grow into normal size, and cysts of onion stage spermatids consisting of 64 sets of nuclei and nebenkerns are clearly observed (data not shown). To better visualize putative spermatogenesis defects of dfxr mutants, we crossed into the dfxr^{50M} null mutant background a GFP transgenic marker line, DJ-GFP, under the control of the endogenous DJ promoter, which specifically labels spermatid bundles after the individualization process has been initiated (Santel et al., 1998). Comparison of age-matched control and dfxr null mutants (<12 h after eclosion) revealed spermatid bundles elongated to the normal length in both genotypes, however, the conspicuous coiled spermatid bundles located at the testis base were specifically missing in the dfxr mutants (compare Figs. 4A and 4C). This observation was confirmed under Nomarski optics (compare Figs. 4B and 4D). Instead of the mature spermatids, degenerated cell debris, appearing as granules under Nomarski optics,
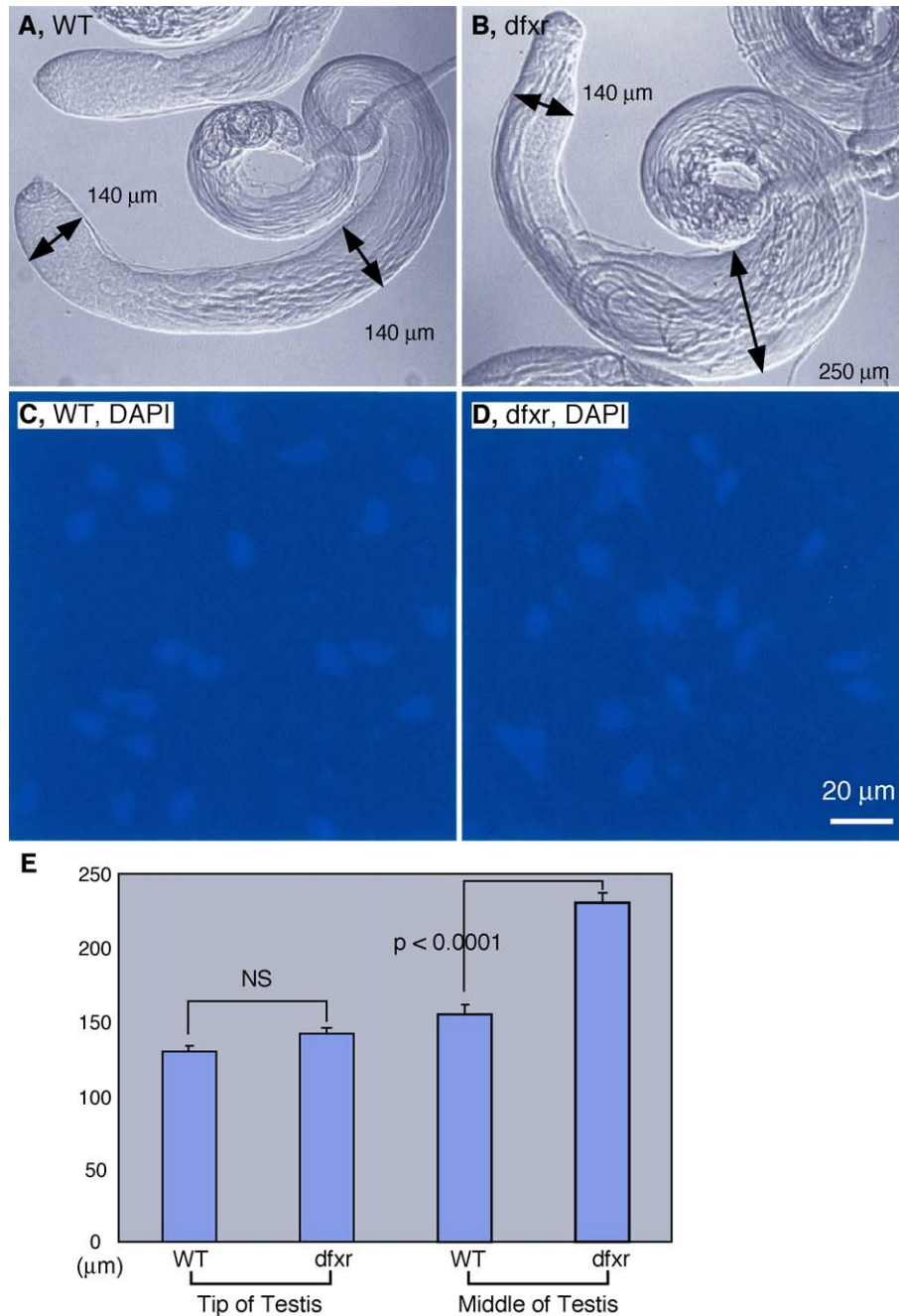
Fig. 3. *dfxr* mutants have enlarged testes. (A, B) Whole-mount testes from adult flies within 12 h after eclosion. The genetic control (WT, A) and homozygous null *dfxr* mutant (*dfxr*[50M], B) are shown. The measurements of testes diameter at the tip and middle of the testes are indicated. (C, D) Nuclear cluster of spermatid cysts from control and mutants are displayed with DAPI staining of testis squashes. The number of spermatid bundles in *dfxr* mutants and controls is indistinguishable. (E) Quantification of testis size of both genotypes at the tip and middle of testes. The diameter at the middle of mutant testes is significantly larger than the control. Mean $\pm$ SEM ($P < 0.0001$; $N > 14$).

fills the base of *dfxr* mutant testes (Fig. 4D). When testes squashes were probed with an α-tubulin antibody, abnormal super-coiled, probably degenerating, spermatids were revealed in the basal testicular region of *dfxr* mutants, which were never observed in control animals (Fig. 4D inset); the degenerating spermatid tangles showed almost no DJ-GFP labeling. As a consequence of this late-stage arrest, *dfxr* mutants of 2–3 days old have only a few individualized

spermatozoa in the seminal vesicles. In contrast, testes from control animals are full of mature spermatozoa stored in the seminal vesicles (compare Figs. 4E and 4F). Similar phenotypes are present in allele *dfmr*[3] (data not shown). The phenotype of empty seminal vesicles and granular debris at the testis base, together with fully elongated spermatid bundles arranged along the length of testis, is reminiscent of defects associated with loss of classical Y chromosome
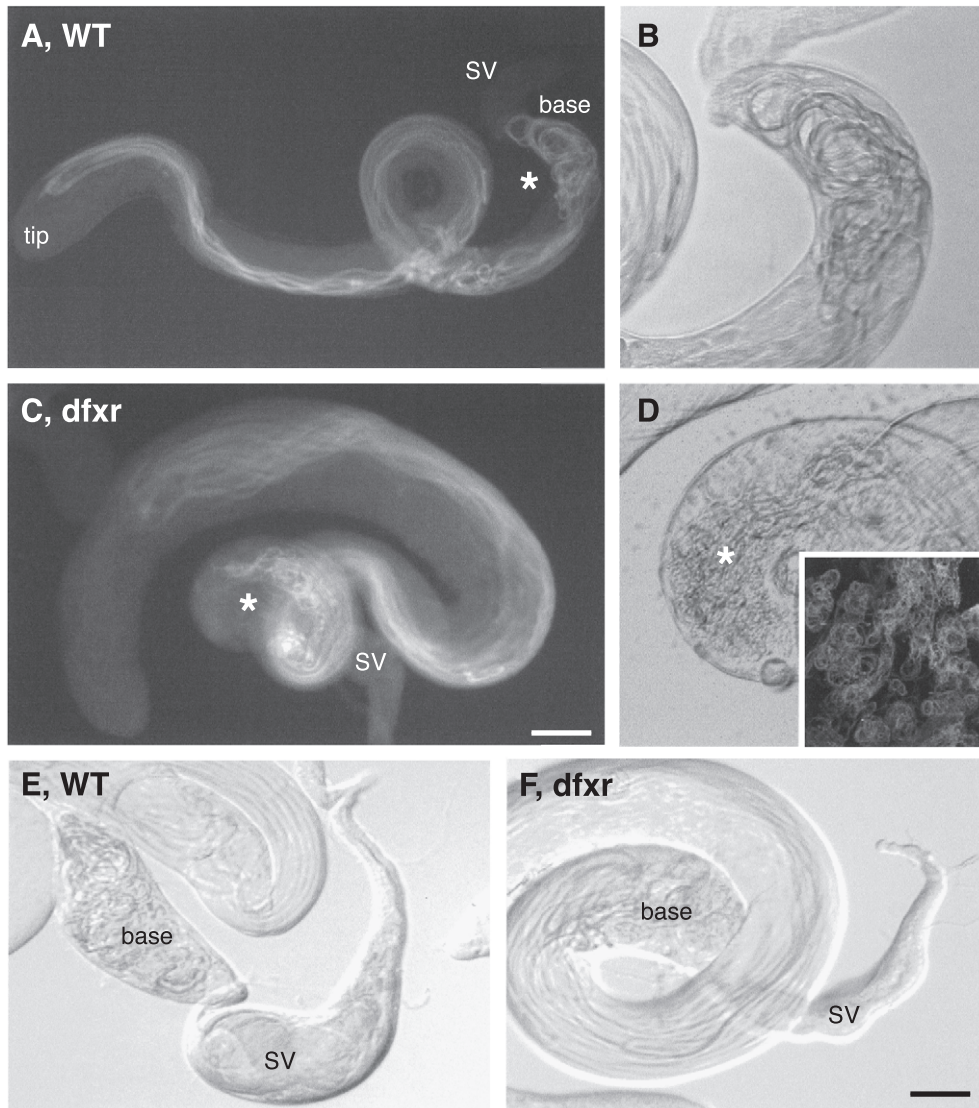
Fig. 4. Late-stage spermatogenesis is defective in *dfxr* mutants. (A) A fluorescent image of a DJ-GFP labeled wild-type testis. The tip, base, and seminal vesicle (SV) of a testis are indicated. Note that only the late-stage spermatid bundles after the individualization process is initiated are revealed by DJ-GFP, as white bundles along the sides of testes. (B) A Nomarski image of the testis base indicated by the asterisk (*) in A. Coiled spermatid bundles ready to move into the SV are clearly observed. (C) A fluorescent image of a DJ-GFP labeled *dfxr*[50M] null mutant testis. Note the obvious enlargement of the mutant testis relative to the wild type (compare A and C). The distribution of late-stage elongated spermatid bundles labeled by GFP in mutants (C) is not as tight as in the wildtype (A). Scale bar: 150 μm. (D) A Nomarski image of the base of mutant testes reveals amorphous structure, rather than coiled bundles in controls (compare D and B). The inset of D shows the spermatid tangles released from the base of mutant testes when squashed, visualized by staining with an anti-tubulin antibody. The spermatid tangles are never seen in controls. (E, F) The testes of 3-day-old flies. The SV is replete with motile spermatozoa in WT (E), but void of spermatozoa in *dfxr* mutants (F).

fertility factors (Hardy et al., 1981; Timakov and Zhang, 2000), some of which are now known to encode dynein heavy chains (Carvalho et al., 2000 and therein).

The individualization process of spermatogenesis in dfxr mutants is largely normal

Spermatid elongation is immediately followed by an actin-dependent individualization process. During individualization, each spermatid within a cyst develops its own plasma membrane and squeezes out excess cytoplasmic

content (Fabrizio et al., 1998). All previously characterized sterile mutants with elongated spermatid cyst have individualization defects (11 mutants; Fabrizio et al., 1998). To pinpoint the late-stage spermatid differentiation defects caused by *dfxr* mutations, we next performed antibody/dye staining on testis squashes.

DAPI staining of *dfxr* mutant testes reveals that spermatid nuclei are condensed, with the normal needle-like morphology and mostly clustered with 2–5 nuclei in each cyst slipped off the main bundle (compare Figs. 5A and 5D). Quantification of total spermatid nuclei clusters indi-
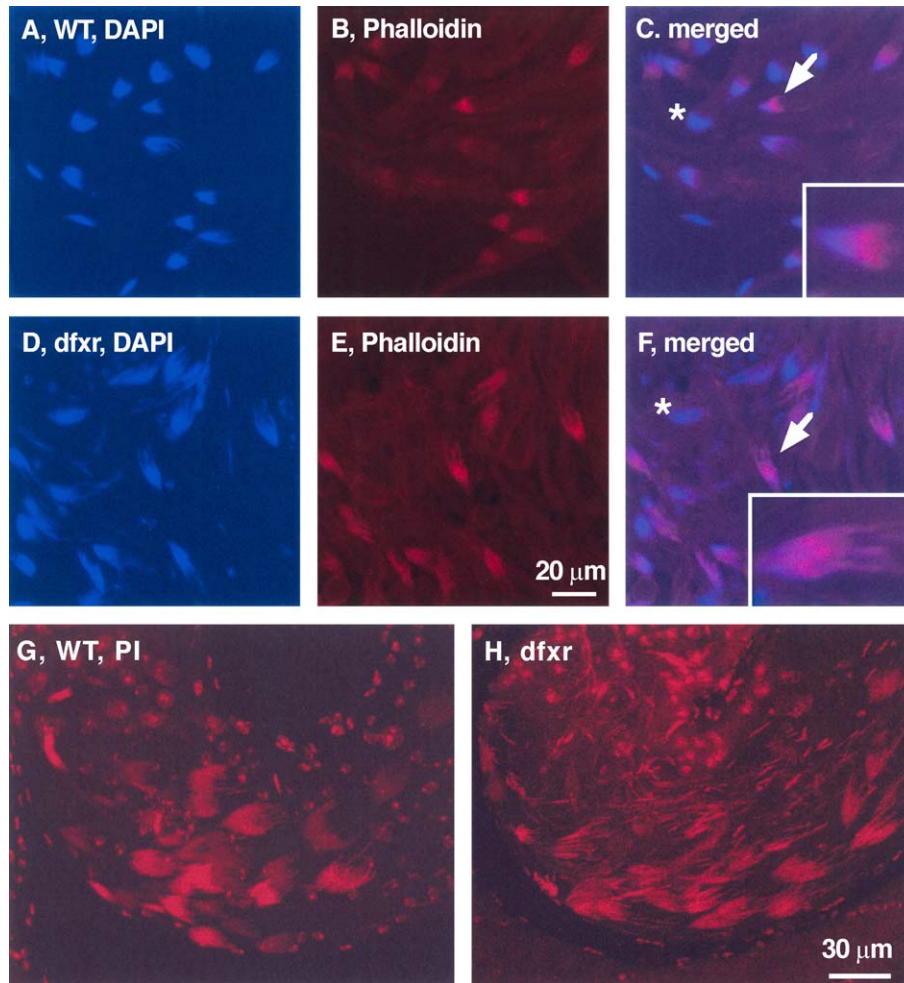
Fig. 5. *dfxr* mutants display a largely normal spermatid individualization process. (A, B) WT spermatid nuclei detected by DAPI staining (A in blue) and the individualization complex stained with Texas-red labeled phalloidin (B in red) of testis squashes. (C) Merged image of A and B. * denotes a cluster of nuclei (in blue) with individualization complex moved away. The arrow shows a spermatid cyst head with nuclei cluster (in blue) at the tip immediately followed by individualization complex (in red); its enlarged view is shown in the inset. (D, E, F) Images of *dfxr* mutants corresponding to wildtype A, B, C, respectively. Note the finger-like structure of 3 spermatid heads slipped off the main cluster. (G, H) Nuclear heads of spermatid cysts revealed by propidium iodide staining of whole-mount WT (G) and mutant (H) testes. The 64 spermatid heads are tightly clustered in WT (G); the vast majority of spermatid nuclei are clustered together with a few slipped off in the mutants (H). The base of testes shown in G and H is to the left; tip to the right.

cates no significant difference between *dfxr* mutants and controls. Texas red phalloidin staining for F-actin similarly shows that the actin-based individualization complex (IC) is largely normal near the spermatid heads, with $2-5$ finger-like structures protruding out of the main complex (compare Figs. 5B and 5E), so do ICs along the length of spermatid bundles and waste bags at the spermatid terminal ends (data not shown). Quantification of total ICs from phalloidin-stained squashes showed that *dfxr* mutants have a mean 20.0 ± 5.56 ICs per testis compared to 20.4 ± 2.88 in controls ($P > 0.8$, $N > 10$). Nuclear staining with propidium iodide on whole-mount testes also showed that nuclei of spermatid cyst are mostly clustered and arranged in normal order (compare Figs. 5G and 5H). These results indicate that the spermatid individualization process is largely normal in *dfxr* mutants, which was confirmed later in ultrastructural analyses (see below). Taken together,

these results indicate an unusually late-stage-specific spermatogenesis arrest in *dfxr* mutants following the spermatid individualization process.

Central pair microtubules of spermatid axoneme are specifically lost in dfxr mutants

Spermatogenesis was next examined at the electron microscope level to investigate the cause of the late-stage spermatid arrest in *dfxr* mutants. Few defects were observed in general spermatid morphology. In confirmation of the light microscope analyses, the spermatid individualization process in mutants appears complete and largely normal in most cases, although occasional individualization defects are observed within a 64 spermatid cyst (data not shown). A clear phenotype (multiple mutant alleles show similar phenotypes, but the results of *dfxr*[50M] is

presented here) is that the orientation of spermatid tails within a cyst is often arranged in an irregular fashion in *dfxr* mutants. In addition, the configuration of mitochondria and axoneme within a sperm flagellum is variably skewed, as well as some unknown ring structures present at the inter-space between spermatid tails which is not seen in controls (Figs. 6A and 6B). However, by far, the most revealing phenotype is a specific disruption of the microtubule axoneme structure in the sperm flagellum which becomes progressively more pronounced as spermatid differentiation proceeds.

The newly formed sperm tail axoneme has a simple "9 + 2" microtubule configuration of 9 outer microtubule doublets and a central pair of microtubules (Fig. 6C). As the axoneme develops, more and more accessory proteins are

added to this core microtubule structure, giving the axoneme its characteristic pinwheel cross-section (Fig. 6C). A highly characteristic *dfxr* mutant phenotype is the loss of the central pair microtubules without other discernable defects associated with overall axoneme integrity. The axonemes of mutant sperm tails always maintain the normal outer microtubule doublet ring, but some have a clearly empty center, demonstrating the specific loss of central pair microtubules (compare Figs. 6C and 6D). Interestingly, the loss of central pair microtubules is progressive during spermatid differentiation. In early-stage spermatids, 30% have the central microtubule pair missing (over 200 spermatids scored), whereas the frequency of this defect has doubled in late-stage spermatids with 56.5% lacking the central pair (Fig. 6E). The presence of normal-appearing spermatids in a cyst is consistent with
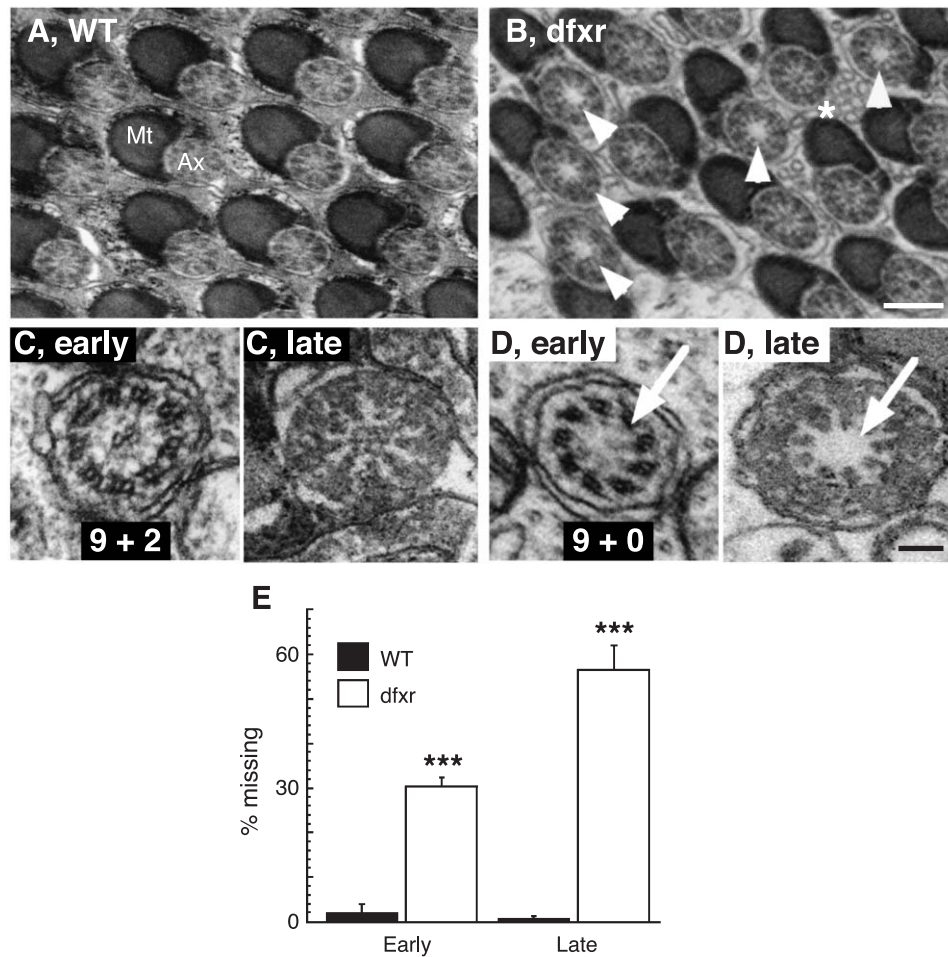
Fig. 6. The central pair of microtubules in the spermatid axoneme of *dfxr* mutants is lost progressively during spermatogenesis. (A, B) Cross-sections of a late-stage spermatid cyst from wildtype OR (A) and *dfxr* mutant allele *dfxr*[50M] (B). At this stage, a sperm tail consists of electron dense mitochondria (Mt) and electron light axoneme (Ax). Arrows in B point to the empty center of axonemes in the mutant. * indicates ring structure in mutants not observed in controls. Scale bar: 200 nm. (C) High-resolution images of wild-type axonemes during early- and late-stage spermatogenesis. The early-stage flagellum is characterized by a simple configuration of nine outer pairs of microtubules and one central pair of microtubules without obvious accessory structures. The late-stage flagellum contains the 9 + 2 microtubule configuration with extensive accessory structures. (D) Comparable images from early- and late-stage *dfxr* mutant spermatids. Arrows point to the empty center of axonemes with central pair of microtubules missing. Scale bar: 80 nm. (E) Quantifications of the percentage of axonemes with the central pair of microtubules absent. Early- and late-stage spermatids are defined the same way as in C and D. Mean ± SEM (*** denotes $P < 0.001$ by Student's t test).

the residual fertility observed in *dfxr* mutants. To our knowledge, the progressive loss of central pair microtubules have not been previously reported in any other *Drosophila* sterile mutants and is specific to the loss of dFXR.

dFXR requirement in sperm axoneme development is not mediated by Futsch

In the nervous system, dFXR also plays a role in regulating microtubule dynamics by suppressing the translation of Futsch (Zhang et al., 2001). Decreased Futsch expression (hypomorphic *futsch*[N94] allele) is sufficient to restore normal neuronal function in *dfxr* null mutants. *dfxr*, *futsch* double mutants display synaptic structure and function indistinguishable from controls (Zhang et al., 2001). Given the similarity of the structural defects involving microtubules in sperm axoneme and neurons, it was essential to examine whether a common molecular mechanism

mediates the *dfxr* requirement during spermatogenesis. Wild-type testes were stained with a specific monoclonal antibody 22C10 (from Iowa Hybridoma Bank) against Futsch. The Futsch protein was not present in spermatogonia or spermatocyte cells, although readily detectable expression was observed in neurons innervating the testes (data not shown). Consistent with absence of Futsch expression in testes, *futsch* plays no role in male fertility. Null *futsch* mutants are embryonic lethal, but a viable hypomorph (*futsch*[N94]) shows no defects in male fertility (data not shown). Finally, *dfxr*[50M], *futsch*[N94] double mutants had fertility comparable to the *dfxr*[50M] mutant alone, and no fertility rescue was observed (data not shown). Taken together, these data fail to indicate any prospect that Futsch mediates the dFXR requirement during spermatogenesis, suggesting that the molecular mechanism-mediating axoneme microtubule stability in the testes is distinctive from the Futsch-dependent neuronal mechanism.
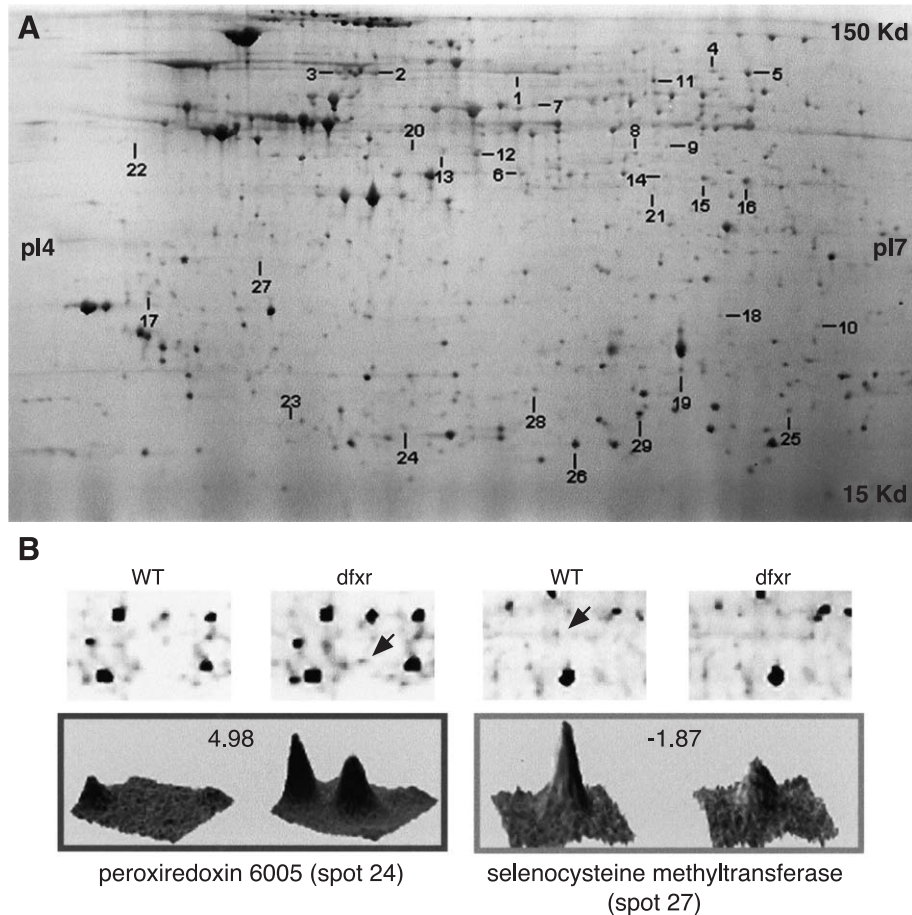
Fig. 7. Proteomic analyses of *dfxr* mutant testes reveal proteins with altered abundance. (A) Representative 2D electrophoresis gel post-stained with Sypro Ruby. The iso-electronic focusing range was from PI 4 to 7 (left–right); protein size range from 15 to 150 kDa (bottom-up). The protein spots (29 in total) identified to have significantly changes of abundance in mutants are indicated. (B) Expression alterations of two representative proteins in *dfxr* mutants. Upper row shows corresponding pairs of gel blocks containing the interest of protein (shown by an arrow) with altered abundance in mutants. The black and white images were converted from fluorescence-labeled samples. Lower row shows volume change computed from fluorescence intensity. Peroxiredoxin 6005 (left panel) has a 4.98-fold increase of abundance in mutants; selenocysteine methyltransferase (right panel) a 1.87-fold decrease. WT denotes *FRT82B* control flies; dfxr denotes *FRT82B*; *dfxr*[50M] homozygous mutants.

DIGE proteomic analyses reveal protein expression alterations in dfxr mutant testes

It is well established that FMRP/dFXR binds mRNA and functions as a translational regulator (Brown et al., 2001; Jin and Warren, 2000; Li et al., 2001; Schaeffer et al., 2001; Zhang et al., 2001). This indicates that dFXR is most likely required for spermatogenesis because it regulates the translation of proteins essential for flagellar development and axoneme stability. We therefore set out to identify the proteins whose expression is altered in the testes of *dfxr* mutants, taking a systematic proteomics approach. As shown above, immotile mutant spermatids eventually degenerated after individualization. Therefore, testes were dissected from freshly eclosed (<12 h) adult animals from genetic controls and *dfxr* null mutants. Three independent pairs of control and mutant samples were individually labeled with fluorescent dyes Cy3 and Cy5, respectively. Each labeled pair was assayed on a separate 2D gel, along with a Cy2-labeled mixture of all six samples to allow for statistical comparison of protein abundance changes for individual proteins across all three replicates. All protein spots with a significant difference were identified by mass spectrometry and database interrogation against the *Drosophila* genome.

Two-dimensional difference gel electrophoresis (2D DIGE) is a newly developed proteomics technology that overcomes many of the caveats of conventional 2D gel analysis; it employs various external and internal controls and multiple sampling as shown above such that changes in protein abundance can be detected with statistical confidence (Alban et al., 2003; Friedman et al., 2004). Overall, the protein expression patterns of control and *dfxr* null mutant testes were surprisingly similar (Fig. 7), with only a handful of protein groups showing any significant alterations. Approximately 1500 protein spots with isoelectric points between pH 4 and 7, and molecular weights between 15 and 150 kDa were resolved on these gels (Fig. 7A). Twenty-nine protein spots representing 23 distinct proteins (redundancy due to post-translational modification) showed significant changes ($P < 0.05$ using Student's t test) when quantified across the three independent experiments (Fig. 7 and Table 1). Of these 29 identified features, 11 have significantly decreased expression and 18 have significantly increased expression in *dfxr* null mutants compared to control testes. Extending this assay to the entire testes proteome, loss of dFXR function causes a detectable misregulation of <2% of the total protein species in the testes. This finding argues that dFXR plays a selective role in translational regulation in the testes and is not a general translational regulator, consistent with the tight specificity of the developmental arrest of spermatogenesis in the *dfxr* mutants.

Proteins that are misregulated in the *dfxr* mutant testes can be categorized into just five functional groups (Table 1), (1) Hsp chaperone/protein folding (four proteins), (2) protein/DNA turnover proteins (three proteins), (3) glycolysis

Table 1
Proteins with altered expression profiles in *dfxr* mutant testes

Hsp and protein folding		Protein/DNA metabolism	
Hsp68, 1	−1.32**	ubiquitin-like/	1.62*
Hsp60B, 2/3	−1.94**,	CG11139, 20	
	3.9**	COP9 signalosome	2.16**
Hsp90-related protein	1.32*,	subunit 4, 21	
TRAP1, 4/5	1.42*	Rad23, DNA	3.06*
FKBP59, 6	1.27*	repair protein, 22	
Glycolysis		*Redox and ion homeostasis*	
Hexokinase A, 7	−1.31*		
Isocitrate dehydrogenase, 8	1.35**	peroxiredoxin	−5.96**,
Phosphopyruvatehydratase, 9	1.38*	6005, 23/24	4.98**
Walrus, an electron	−1.29**	peroxiredoxin	−2.16*
carrier, 10		2540, 25	
		thioredoxin	1.26*
Miscellaneous		peroxidase, 26	
Mitochondria outer	1.44*	selenocysteine	−1.87**
membrane translocase		methyltransferase, 27	
complex/CG6756, 11		ferritin 1 heavy	1.35*
Gdi-related (gi|18467646),	1.41*,	chain homolog, 28	
12/13	−1.75*	ferritin 2 light	−1.21*
Phosphoethanolamine	1.36*,	chain homolog, 29	
cytidylyltransferase,	1.5*,		
14/15/16	1.5**		
Farnesoic acid	−3.52**		
O-methyltransferase/			
CG10527, 17			
Nitrophenylphosphatase/	1.46*		
CG32487, 18			
SCP-containing protein C, 19−1.49*			

Note: numbers after each entry correspond to the spots shown on the 2D gel (Fig. 7A). Two or more numbers indicate multiple iso-electric variants identified. "+" indicates times of increase compared to controls; "−" times of decrease. In total, there are 23 proteins (29 protein spots, 11 decreased, 18 increased) identified with altered expression patterns in *dfxr* mutant testes.
* $0.05 < P > 0.01$.
** $P < 0.01$.

proteins (four proteins), (4) redox homeostasis proteins (six proteins), and (5) a miscellaneous group of proteins outside these categories (six proteins). Two of these proteins (Hsp90-related protein TRAP1 and phosphoethanolamine cytidylyltransferase) have at least two isoelectric variants changing in the same direction, that is, increased expression. In addition, three of the proteins (Hsp 60B, peroxiredoxin 6005, and Gdi-related protein) have two isoelectric variants changing in opposite directions, consistent with alterations in post-translational modifications (Table 1). Thus, these post-translationally modified proteins are presumed to be indirect downstream targets of dFXR, not directly regulated at the level of translation. The relative significance of these proteins in spermatogenesis has yet to be elucidated. It is important to note that the abundance of all the tubulin isoforms is unaltered in *dfxr* mutant testes, suggesting that the loss of axoneme integrity is a microtubule stability defect, rather than direct loss of tubulin proteins. It is also particularly noteworthy that members of the first group of proteins, that is, chaperone proteins Hsp60B and Hsp90, have been previously implicated in microtubule stability and

Drosophila spermatogenesis (Timakov and Zhang, 2000; Yue et al., 1999).

fmr1 knockout mice display late-stage-specific, malformed spermatids

Enlarged testes are present in FraX patients, *fmr1* knockout mice (Bakker et al., 1994), and *Drosophila dfxr* null mutants (this report). Similarly, late-stage spermatid malformation was found in patients (Johannisson et al., 1987) and flies (this report). These similarities suggest that dFXR/FMRP may play a conserved role in spermatogenesis across species. We therefore performed a comparative analysis of fertility and spermatogenesis in the *fmr1* knockout mice to determine whether the mutant phenotypes documented above in flies are also apparent in mammals. We first confirmed that the fertility of *fmr1* knockout mice in a clean-up FVB background (see Materials and methods) is comparable to controls. Single pair matings were set up between knockout or FVB control males (<3 months) and FVB females (<3 months). The mean litter size of male mutants was 10.3 ± 2.3 pups per male ($N = 10$), similar to control animal litter sizes of 8.3 ± 1.5 pups per male, demonstrating that male *fmr1* mutant mice have normal

fertility, consistent with the original report (Bakker et al., 1994). Given that *dfxr* mutant flies have the conspicuous, specific axonemal defects, we set out to find out if similar defects were present in *fmr1* KO mice, particularly in epididymis where mature spermatozoa are stored. Though initial characterization of *fmr1* KO mice included testes sections examined under light microscope and reported normal morphology (Bakker et al., 1994), an examination of spermatogenesis under electron microscopy has never before been done. Our histological analyses showed no apparent testicular or early-stage spermatogenesis defects in mutant testes (data not shown) consistent with the published results (Bakker et al., 1994). In contrast, electron microscopy showed an obvious scarcity of spermatids in mutant testes compared to controls, and more so of mature spermatids in epididymis (compare Figs. 8A and 8B). The scarcity of spermatids observed in KO mice is reminiscent of "reduced spermatogenesis" reported in 10 patients published from four laboratories in the 1970s and 1980s of last century (Johannisson et al., 1987 and therein). These results indicate that FMRP plays a role in mammalian spermatogenesis.

At high resolution, although apparently normal spermatids were observed in *fmr1* knockout mice, two types of
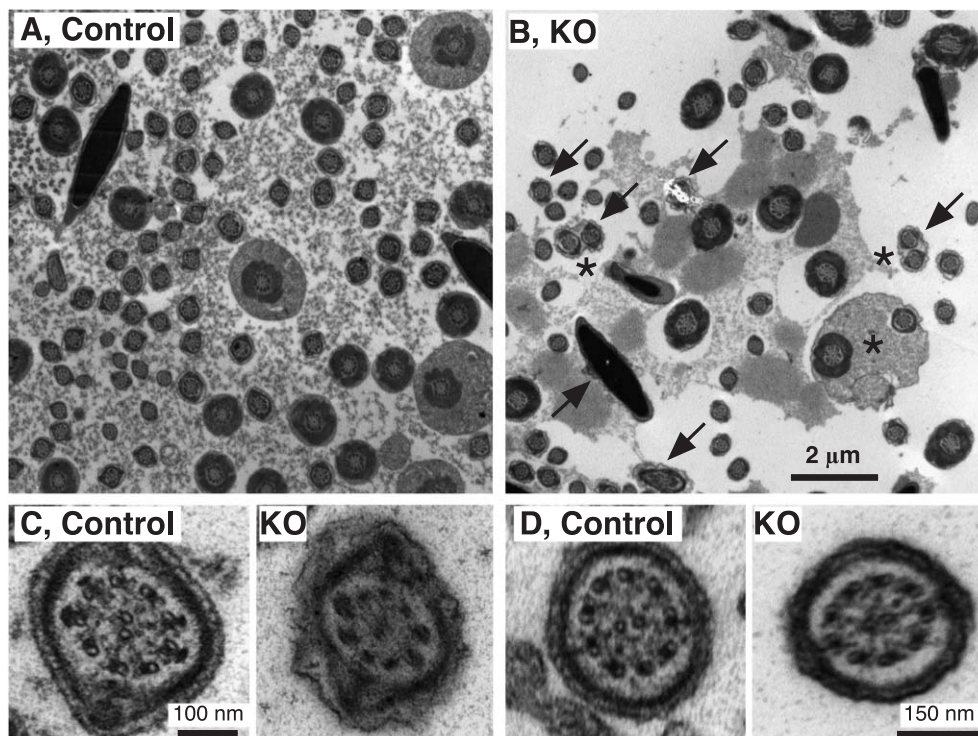
Fig. 8. *fmr1* knockout mice have fewer and malformed spermatids. (A, B) Representative electron microscope micrographs of spermatids from the epididymis of control FVB mice (A) and *fmr1* knockout (KO) mouse (B). Spermatids in the mutant epididymis are always markedly less abundant compared to controls. In panel B, arrows denote spermatids with wavy form of plasma membranes; * denotes two spermatids sharing the same plasma membrane. (C, D) Specific segments of individual spermatids at higher resolution. A comparison of control and mutant principal pieces is shown in C and end pieces in D. Mutant spermatids show compromised membrane integrity, with the membrane malformed and variably disassociated from underlying dense fibers. Mutants consistently display poorly defined axoneme structure (KOs in C and D), compared to the crisp resolution of the 9 + 2 microtubule arrangement in controls (controls in C and D). These ultrastructural defects were routinely obvious in mutant processed in parallel with control spermatozoa from testes and epididymis.

abnormalities were obvious in >80% of spermatids examined in testes and more so in epididymis. First, the integrity of the plasma membrane appears defective in *fmr1* mutant spermatids. In controls, the spermatid membrane is always smooth and closely associated with underlying dense fibers, whereas the mutant membranes are variably distorted, wavy, and disassociated from the sperm tail axoneme (Fig. 8C). This defect is observed along the length of the spermatid, but most pronounced in the principal piece (Figs. 8C). Similar wavy membrane was reported in a patient (Fig. 5e of Johannisson et al., 1987; no information about axoneme structure in patients is available in literature). Second, although the 9 + 2 axoneme structure is usually maintained in mutant spermatids, the organization and/or stability of the microtubule array is clearly compromised. In control axonemes, the microtubules form pairs of tubulin rings of uniform size that are crisply defined in EM cross-section (controls in Figs. 8C and 8D). In contrast, *fmr1* mutant axonemes display a variably perturbed microtubule ring structure and the protein lattice lacks clear definition (KO in Figs. 8C and 8D). This observation was made repeatedly in testes from five mutant mice processed and imaged in parallel with controls, and therefore does not represent an experimental artifact. Rather, the mutant axoneme integrity appears consistently compromised. The phenotypic difference between mutant flies (central pair microtubules missing) and KO mice (compromised axonemal integrity) may reflect the fact that three FMRP family proteins are present in overlapping patterns in the mouse testes, and only one of these is removed in the KO mice. The likelihood of overlapping functions in spermatogenesis between these FMRP family members is supported by the fact that double knockout mice of *fmr1* and *fxr2* are sterile (D. Nelson, personal communication), similar to the *Drosophila dfxr* mutant alone. Taken together, this work suggests that dFXR/FMRP has a conserved role in maintaining axoneme structure and stability in fruitflies and mammals.

Discussion

Drosophila has long served as a genetic model system for spermatogenesis, through the isolation and characterization of male sterile mutants to reveal molecular mechanisms (Castrillon et al., 1993; Fabrizio et al., 1998; for reviews, see Fuller, 1993; Lindsley and Tokuyasu, 1980). Majority (approximately 70%) of the *Drosophila* male sterile mutants has been found to disrupt spermatogenesis postmeiotically (Castrillon et al., 1993), and all 11 mutants examined by Fabrizio et al. (1998) display spermatid individualization defects. Among many sterile mutants characterized so far, only two genes have defects restricted to stages following the spermatid individualization stage, *kl-3* (γ dynein) and *kl-5* (β dynein), which encode proteins with roles in axoneme integrity and function (Timakov and Zhang, 2000). The other male sterile mutants, including tubulin and its inter-

acting gene mutants, have widespread spermatogenesis defects encompassing phenotypes from meiosis through to late-stage axoneme assembly (Kemphues et al., 1980; Regan and Fuller, 1988, 1990). It is therefore most intriguing that *dfxr* mutants show a highly specific phenotype limited to late stage of spermatogenesis after individualization. This phenotype is most reminiscent of dynein heavy chain *kl-3* and *kl-5* mutants (Zhang and Stankiewicz, 1998). Indeed, *dfxr*, *kl-3*, and *kl-5* are the only genes characterized so far to affect exclusively the post-individualization process of spermatogenesis. It is interesting to note that both dynein and dFXR contribute to the structural integrity of the sperm tail axoneme.

The axoneme "9 + 2" microtubule configuration of nine outer doublets and a single central pair is one of the most familiar, conserved ultrastructure features across different species. In *dfxr* mutant spermatids, the central pair microtubules are specifically lost, while the outer ring microtubule doublets are not detectably altered, generating a characteristic "9 + 0" profile within the mutant sperm tail. Interestingly, the central pair is lost gradually during the progression of spermatogenesis. In early axoneme formation, approximately 70% of the spermatids contain a normal 9 + 2 flagellar axoneme, but the frequency of central pair loss approximately doubles as spermatogenesis proceeds. This suggests that, at least in many cases, the axoneme is initially formed normally but then the central pair of microtubules is lost due to a lack of stability. The central pair of microtubules is not required for spermatid elongation, but required for spermatid coiling, as coiled sperm bundles are absent in *dfxr* mutant testes. It is plausible that the coiling process requires axoneme movement to retract the sperm tails from the testis tip to the base. The central pair is clearly required for the motility of flagella (for review, see Smith and Lefebvre, 1997) and so provides a mechanistic explanation for the impaired male fertility.

What could cause the specific loss of the central microtubule pair while leaving the outer microtubule ring intact? Only a few other mutants and perturbations have been reported to result in this specific defect. Occasionally, the central pair of microtubules is reported missing in the *Drosophila whirligig* mutant (product unknown), which interacts genetically with β-tubulin mutants, but *whirligig* mutants have additional, more complex spermatogenesis phenotypes (Green et al., 1990). In sea urchins, shorter and immotile "9 + 0" ciliary axonemes are produced when anti-kinesin II antibody is injected into fertilized eggs, suggesting that Kinesin II might play a similar role to dFXR in axoneme maturation/stabilization (Morris and Scholey, 1997). Most interestingly, in *Drosophila*, the carboxyl terminal of $\beta2$-tubulin is critical for the assembly of the central pair of microtubules. In particular, the amino acid residues EG at 433–434 appear to mediate the selective assembly of just the central pair microtubules (Nielsen et al., 2001; Raff et al., 2000). Similarly, the absence of central pair microtubules has been reported in

Tetrahymena when the carboxyl terminal polyglycylation domain of β-tubulin is mutated (Thazhath et al., 2002). This domain is part of the "axoneme motif" identified in *Drosophila* (Nielsen et al., 2001). Thus, a mechanism involving post-translational modification of β2-tubulin is specifically required for the integrity of central pair of microtubules in the sperm axoneme. At a minimum, these studies demonstrate that the central pair of microtubules is regulated independently of the outer ring doublets in the sperm flagellum. The dFXR protein may be required in one of these mechanisms or in an unknown distinctive specific mechanism which stabilizes the central pair of microtubules during axoneme development.

dFXR as a translational regulator during spermatogenesis

Extensive studies from flies to mammals show that translational control plays a critical role in spermatogenesis. Before meiosis, transcripts are held in an inactive form, whereas following meiosis massive translation occurs to accommodate the dramatic morphogenetic changes during spermatid differentiation (for reviews, see Schafer et al., 1995; Venables and Eperon, 1999). A number of RNA-binding proteins have been identified as translational regulators during spermatogenesis in both vertebrates and invertebrates; some of those functionally characterized act as translational repressors (Venables and Eperon, 1999). For example, *Drosophila* testis-specific RNA recognition motif protein (TSR) and mouse Prm-1 RNA binding protein (Prbp) are negative translational regulators required to block translation until the appropriate stage of spermatogenesis (Haynes et al., 1997; Lee et al., 1996). However, the functional mechanisms and spermatogenesis defects of other RNA-binding proteins, such as ribonuclear protein at 97D (RB97D; Heatwole and Haynes, 1996) and P element somatic inhibitor (PSI; Labourier et al., 2002), have not been well established. This study shows that dFXR is a new class of RNA-binding protein required for spermatogenesis.

It is well established that both dFXR and FMRP mediate their effects as translational regulators, in many cases as negative regulators (Brown et al., 2001; Laggerbauer et al., 2001; Li et al., 2001; Miyashiro et al., 2003; Zhang et al., 2001), but in other cases as positive regulators (Brown et al., 2001; Miyashiro et al., 2003). In the nervous system, dFXR acts as a negative regulator of Futsch (MAP1B) translation to control microtubule stability (Zhang et al., 2001). Although this role has obvious parallels with the dFXR-mediated microtubule assembly/stability during spermatogenesis, there is no evidence that Futsch plays any role in the testes. This suggests that dFXR has a similar role in regulating the microtubule cytoskeleton in both sperm and neurons, but must operate via a distinctive translation regulation mechanism in the different cell types. In the absence of any identified, or likely, dFXR targets in the testes, we turned to a proteomics approach to identify proteins whose level is altered in *dfxr* mutant testes. Given the hundreds of putative FMRP targets identified in neurons identified by microarray analyses (Brown et al., 2001; Miyashiro et al., 2003), it was a pleasant surprise to discover that only a very few proteins (<2% of the proteins resolved by the 2D gel conditions used) were significantly altered in *dfxr* mutant testes. Among the proteins with altered expressions, some increased in level and others decreased. Of the 29 protein species significantly altered, only 11 showed a change of protein abundance of > 1.5-fold (increase or decrease). The small group of proteins altered in expression levels identified in the DIGE analyses does not intuitively explain the molecular basis of the axoneme defect in *dfxr* mutants. However, several identified proteins are known or suggested to be involved in spermatogenesis, including Hsp60B (Timakov and Zhang, 2000), hexokinase (Mori et al., 1998), peroxiredoxin (Sasagawa et al., 2001), and components of the ubiquitin pathway (Orgad et al., 2000). Most interestingly, Hsp60B is essential for male fertility in *Drosophila* due to its role in late-stage spermatid differentiation (Timakov and Zhang, 2000). Though mutants for Hsp90-related protein TRAP1 have not been generated in any organism, mutations in the *Drosophila* Hsp90 chaperone result in male sterility (Yue et al., 1999). Hsp90 mutants show microtubule defects at all stages of spermatogenesis including defective membrane structures and axonemes (Yue et al., 1999). This role has obvious parallels to the function of dFXR reported here.

Like any method, a proteomics screen is limited in scope and will not reveal all possible protein targets of dFXR regulation. In particular, the experiments presented here are limited to revealing more abundant proteins with isoelectric points between pH 4–7 and molecular weights between about 15 and 150 kDa. This leaves open the possibility for additional dFXR targets which are either too low in abundance to be detected, or have characteristics that fall outside of this screening range. Moreover, the *dfxr* mutation results in late spermatid arrest and eventual degeneration. Although we were very careful to collect testes only from newly eclosed young males (<12 h) before any detectable spermatid degeneration, the presence of stressed cells could have contributed to the identification of protein/DNA turnover proteins and redox/homeostasis proteins in the mutant testes. Nevertheless, this innovative proteomics approach has identified intriguing putative targets or pathways, which represent probable targets for dFXR regulation. These proteins provide the lead to assay putative genetic interaction with dFXR, via forward and reverse genetic approaches, as well as to identify novel functions for these proteins in spermatogenesis.

Future directions

Drosophila dfxr mutants exhibit late-stage-specific spermatogenesis defects, a feature also present in human patients and shown here in *fmr1* knockout mice, suggesting

that Fragile X proteins have a conserved function across species during spermatogenesis. The finding that *dfxr* is required for *Drosophila* spermatogenesis has two practical benefits for the study of general FMRP function and the quest to combat FraX. First, spermatogenesis provides an alternative, tractable model system to study the fundamental functions of the dFXR/FMRP family. The neuronal defects associated with *fmr1* knockout mouse and *dfxr* mutant flies are generally subtle and therefore relatively difficult to study. In contrast, this study shows that *dfxr* mutants have a conspicuous, highly specific spermatogenesis defect that causes near complete sterility, facilitating a detailed molecular and genetic study of the dFXR requirement. Second, the male sterility of *dfxr* mutants can be efficiently exploited to mount a large-scale genetic screen. In contrast, no comparable screens present themselves from the subtle, non-essential functions of dFXR in the nervous system (Dockendorff et al., 2002; Morales et al., 2002; Zhang et al., 2001), which would involve more tedious and complicated screening assays. Thus, this study paves the way to dFXR interaction screens based on the readily recognizable sterility phenotype, which will reveal the requirement of dFXR in microtubule stability during axoneme development and, hopefully, illuminate its parallel functions within neurons.

Acknowledgments

References

Alban, A., David, S.O., Bjorkesten, L., Andersson, C., Sloge, E., Lewis, S., Currie, I., 2003. A novel experimental design for comparative two-dimensional gel analysis: two-dimensional difference gel electrophoresis incorporating a pooled internal standard. Proteomics 3 (1), 36–44.

Bachner, D., Steinbach, P., Wohrle, D., Just, W., Vogel, W., Hameister, H., Manca, A., Poustka, A., 1993. Enhanced Fmr-1 expression in testis. Nat. Genet. 4, 115–116.

Bakker, C., Verheij, C., Willemsen, R., vander Helm, R., Oerleman, F., Vermey, M., Bygrave, A., Hoogeveen, A., Oostra, B., Reyniner, E., et al., 1994. Fmr1 knockout mice: a model to study fragile X mental retardation. The Dutch-Belgian Fragile X Consortium. Cell 78, 23–33.

Brown, V., Jin, P., Ceman, S., Darnell, J.C., O'Donnell, W.T., Tenenbaum, S.A., Jin, X., Feng, Y., Wilkinson, K.D., Keene, J.D., et al., 2001. Micro-

array identification of FMRP-associated brain mRNAs and altered mRNA translational profiles in fragile X syndrome. Cell 107, 477–487.

Cantu, J.M., Scaglia, H.E., Medina, M., Gonzalez-Diddi, M., Morato, T., Moreno, M.E., Perez-Palacios, G., 1976. Inherited congenital normo-functional testicular hyperplasia and mental deficiency. Hum. Genet. 33, 23–33.

Carvalho, A.B., Lazzaro, B.P., Clark, A.G., 2000. Y chromosomal fertility factors kl-2 and kl-3 of *Drosophila melanogaster* encode dynein heavy chain polypeptides. Proc. Natl. Acad. Sci. U. S. A. 97, 13239–13244.

Castrillon, D.H., Gonczy, P., Alexander, S., Rawson, R., Eberhart, C.G., Viswanathan, S., DiNardo, S., Wasserman, S.A., 1993. Toward a molecular genetic analysis of spermatogenesis in *Drosophila melanogaster*: characterization of male-sterile mutants generated by single P element mutagenesis. Genetics 135, 489–505.

Darnell, J.C., Jensen, K.B., Jin, P., Brown, V., Warren, S.T., Darnell, R.B., 2001. Fragile X mental retardation protein targets G quartet mRNAs important for neuronal function. Cell 107, 489–499.

Devys, D., Lutz, Y., Rouyer, N., Bellocq, J.P., Mandel, J.L., 1993. The FMR-1 protein is cytoplasmic, most abundant in neurons and appears normal in carriers of a fragile X premutation. Nat. Genet. 4, 335–340.

Dockendorff, T.C., Su, H.S., McBride, S.M., Yang, Z., Choi, C.H., Siwicki, K.K., Sehgal, A., Jongens, T.A., 2002. *Drosophila* lacking dfmr1 activity show defects in circadian output and fail to maintain courtship interest. Neuron 34, 973–984.

Fabrizio, J.J., Hime, G., Lemmon, S.K., Bazinet, C., 1998. Genetic dissection of sperm individualization in *Drosophila melanogaster*. Development 125, 1833–1843.

Friedman, D.B., Hill, S., Keller, J.W., Merchant, N.B., Levy, S.E., Coffey, R.J., Caprioli, R.M., 2004. Proteome analysis of human colon cancer by two-dimensional difference gel electrophoresis and mass spectrometry. Proteomics 4 (3), 793–811.

Fuller, M.T., 1993. Spermatogenesis. In: Bate, M., Afonso, M. (Eds.), The development of *Drosophila melanogaster*. Cold Spring Harbor Laboratory Press, Cold Spring Harbor, New York, pp. 71–147.

Green, L.L., Wolf, N., McDonald, K.L., Fuller, M.T., 1990. Two types of genetic interaction implicate the whirligig gene of *Drosophila melanogaster* in microtubule organization in the flagellar axoneme. Genetics 126, 961–973.

Hardy, R.W., Tokuyasu, K.T., Lindsley, D.L., 1981. Analysis of spermatogenesis in *Drosophila melanogaster* bearing deletions for Y-chromosome fertility genes. Chromosoma 83, 593–617.

Haynes, S.R., Cooper, M.T., Pype, S., Stolow, D.T., 1997. Involvement of a tissue-specific RNA recognition motif protein in *Drosophila* spermatogenesis. Mol. Cell. Biol. 17, 2708–2715.

Heatwole, V.M., Haynes, S.R., 1996. Association of RB97D, an RRM protein required for male fertility, with a Y chromosome lampbrush loop in *Drosophila* spermatocytes. Chromosoma 105, 285–292.

Hinds, H.L., Ashley, C.T., Sutcliffe, J.S., Nelson, D.L., Warren, S.T., Housman, D.E., Schalling, M., 1993. Tissue specific expression of FMR-1 provides evidence for a functional role in fragile X syndrome. Nat. Genet. 3, 36–43.

Huot, M.E., Mazroui, R., Leclerc, P., Khandjian, E.W., 2001. Developmental expression of the fragile X-related 1 proteins in mouse testis: association with microtubule elements. Hum. Mol. Genet. 10, 2803–2811.

Inoue, S., Shimoda, M., Nishinokubi, I., Siomi, M.C., Okamura, M., Nakamura, A., Kobayashi, S., Ishida, N., Siomi, H., 2002. A role for the *Drosophila* fragile X-related gene in circadian output. Curr. Biol. 12, 1331–1335.

Jacobs, P.A., Glover, T.W., Mayer, M., Fox, P., Gerrard, J.W., Dunn, H.G., Herbst, D.S., 1980. X-linked mental retardation: a study of 7 families. Am. J. Med. Genet. 7, 471–489.

Jin, P., Warren, S.T., 2000. Understanding the molecular basis of fragile X syndrome. Hum. Mol. Genet. 9, 901–908.

Johannes, H.P., Hochstenbach, R., Pearson, P.L., 2000. Towards an understanding of the genetics of human male infertility: lessons from flies. Trends Genet. 16, 565–572.

Johannisson, R., Rehder, H., Wendt, V., Schwinger, E., 1987. Spermato-

genesis in two patients with the fragile X syndrome. I. Histology: light and electron microscopy. Hum. Genet. 76, 141–147.

Kemphues, K.J., Raff, E.C., Raff, R.A., Kaufman, T.C., 1980. Mutation in a testis-specific beta-tubulin in *Drosophila*: analysis of its effects on meiosis and map location of the gene. Cell 21, 445–451.

Labourier, E., Blanchette, M., Feiger, J.W., Adams, M.D., Rio, D.C., 2002. The KH-type RNA-binding protein PSI is required for *Drosophila* viability, male fertility, and cellular mRNA processing. Genes Dev. 16, 72–84.

Laggerbauer, B., Ostareck, D., Keidel, E.M., Ostareck-Lederer, A., Fischer, U., 2001. Evidence that fragile X mental retardation protein is a negative regulator of translation. Hum. Mol. Genet. 10, 329–338.

Lee, K., Fajardo, M.A., Braun, R.E., 1996. A testis cytoplasmic RNA-binding protein that has the properties of a translational repressor. Mol. Cell. Biol. 16, 3023–3034.

Li, Z., Zhang, Y., Ku, L., Wilkinson, K.D., Warren, S.T., Feng, Y., 2001. The fragile X mental retardation protein inhibits translation via interacting with mRNA. Nucleic Acids Res. 29, 2276–2283.

Lindsley, D.L., Tokuyasu, K.T., 1980. Spermatogenesis. In: Ashburner, M., Wright, T.R.F. (Eds.), The genetics and biology of *Drosophila*. Academic Press, London, pp. 225–294.

Malter, H.E., Iber, J.C., Willemsen, R., de Graaff, E., Tarleton, J.C., Leisti, J., Warren, S.T., Oostra, B.A., 1997. Characterization of the full fragile X syndrome mutation in fetal gametes. Nat. Genet. 15, 165–169.

Meijer, H., de Graaff, E., Merckx, D.M., Jongbloed, R.J., de Die-Smulders, C.E., Engelen, J.J., Fryns, J.P., Curfs, P.M., Oostra, B.A., 1994. A deletion of 1.6 kb proximal to the CGG repeat of the FMR1 gene causes the clinical phenotype of the fragile X syndrome. Hum. Mol. Genet. 3, 615–620.

Miyashiro, K.Y., Beckel-Mitchener, A., Purk, T.P., Becker, K.G., Barret, T., Liu, L., Carbonetto, S., Weiler, I.J., Greenough, W.T., Eberwine, J., 2003. RNA cargoes associating with FMRP reveal deficits in cellular functioning in Fmr1 null mice. Neuron 37, 417–431.

Morales, J., Hiesinger, P.R., Schroeder, A.J., Kume, K., Verstreken, P., Jackson, F.R., Nelson, D.L., Hassan, B.A., 2002. *Drosophila* fragile X protein, DFXR, regulates neuronal morphology and function in the brain. Neuron 34, 961–972.

Mori, C., Nakamura, N., Welch, J.E., Gotoh, H., Goulding, E.H., Fujioka, M., Eddy, E.M., 1998. Mouse spermatogenic cell-specific type 1 hexokinase mHk1-s) transcripts are expressed by alternative splicing from the mHk1 gene and the HK1-S protein is localized mainly in the sperm tail. Mol. Reprod. Dev. 49, 374–385.

Morris, R.L., Scholey, J.M., 1997. Heterotrimeric kinesin-II is required for the assembly of motile 9+2 ciliary axonemes on sea urchin embryos. J. Cell. Biol. 138, 1009–1022.

Nielsen, M.G., Turner, F.R., Hutchens, J.A., Raff, E.C., 2001. Axoneme-specific beta-tubulin specialization: a conserved C-terminal motif specifies the central pair. Curr. Biol. 11, 529–533.

Orgad, S., Rosenfeld, G., Greenspan, R.J., Segal, D., 2000. Courtless, the *Drosophila* UBC7 homolog, is involved in male courtship behavior and spermatogenesis. Genetics 155, 1267–1280.

Raff, E.C., Hutchens, J.A., Hoyle, H.D., Nielsen, M.G., Turner, F.R., 2000. Conserved axoneme symmetry altered by a component beta-tubulin. Curr. Biol. 10, 1391–1394.

Regan, C.L., Fuller, M.T., 1988. Interacting genes that affect microtubule function: the nc2 allele of the haywire locus fails to complement mutations in the testis-specific beta-tubulin gene of *Drosophila*. Genes Dev. 2, 82–92.

Regan, C.L., Fuller, M.T., 1990. Interacting genes that affect microtubule function in *Drosophila melanogaster*: two classes of mutation revert the failure to complement between haync2 and mutations in tubulin genes. Genetics 125, 77–90.

Reyniers, E., Vits, L., De Boulle, K., Van Roy, B., Van Velzen, D., de Graaff, E., Verkerk, A.J., Jorens, H.Z., Darby, J.K., Oostra, B., et al., The full mutation in the FMR-1 gene of male fragile X patients is absent in their sperm. Nat. Genet. 4, 143–146.

Santel, A., Blumer, N., Kampfer, M., Renkawitz-Pohl, R., 1998. Flagellar mitochondrial association of the male-specific Don Juan protein in *Drosophila* spermatozoa. J. Cell. Sci. 111, 3299–3309.

Sasagawa, I., Yazawa, H., Suzuki, Y., Nakada, T., 2001. Stress and testicular germ cell apoptosis. Arch. Androl. 47, 211–216.

Schaeffer, C., Bardoni, B., Mandel, J.L., Ehresmann, B., Ehresmann, C., Moine, H., 2001. The fragile X mental retardation protein binds specifically to its mRNA via a purine quartet motif. EMBO J. 20, 4803–4813.

Schafer, M., Nayernia, K., Engel, W., Schafer, U., 1995. Translational control in spermatogenesis. Dev. Biol. 172, 344–352.

Schurmann, A., Koling, S., Jacobs, S., Saftig, P., Krauss, S., Wennemuth, G., Kluge, R., Joost, H.G., 2002. Reduced sperm count and normal fertility in male mice with targeted disruption of the ADP-ribosylation factor-like 4 (Arl4) gene. Mol. Cell. Biol. 22, 2761–2768.

Slegtenhorst-Eegdeman, K.E., de Rooij, D.G., Verhoef-Post, M., van de Kant, H.J., Bakker, C.E., Oostra, B.A., Grootegoed, J.A., Themmen, A.P., 1998. Macroorchidism in FMR1 knockout mice is caused by increased Sertoli cell proliferation during testicular development. Endocrinology 139, 156–162.

Smith, E.F., Lefebvre, P.A., 1997. The role of central apparatus components in flagellar motility and microtubule assembly. Cell Motil. Cytoskeleton 38, 1–8.

Tamanini, F., Willemsen, R., van Unen, L., Bontekoe, C., Galjaard, H., Oostra, B.A., Hoogeveen, A.T., 1997. Differential expression of FMR1, FXR1 and FXR2 proteins in human brain and testis. Hum. Mol. Genet. 6, 1315–1322.

Thazhath, R., Liu, C., Gaertig, J., 2002. Polyglycylation domain of beta-tubulin maintains axonemal architecture and affects cytokinesis in *Tetrahymena*. Nat. Cell Biol. 4, 256–259.

Timakov, B., Zhang, P., 2000. Genetic analysis of a Y-chromosome region that induces triplosterile phenotypes and is essential for spermatid individualization in *Drosophila melanogaster*. Genetics 155, 179–189.

Venables, J.P., Eperon, I., 1999. The roles of RNA-binding proteins in spermatogenesis and male infertility. Curr. Opin. Genet. Dev. 9, 346–354.

Vollrath, B., Pudney, J., Asa, S., Leder, P., Fitzgerald, K., 2001. Isolation of a murine homologue of the *Drosophila* neuralized gene, a gene required for axonemal integrity in spermatozoa and terminal maturation of the mammary gland. Mol. Cell. Biol. 21, 7481–7494.

Wan, L., Dockendorff, T.C., Jongens, T.A., Dreyfuss, G., 2000. Characterization of dFMR1, a *Drosophila melanogaster* homolog of the fragile X mental retardation protein. Mol. Cell Biol. 20, 8536–8547.

Yue, L., Karr, T.L., Nathan, D.F., Swift, H., Srinivasan, S., Lindquist, S., 1999. Genetic analysis of viable Hsp90 alleles reveals a critical role in *Drosophila* spermatogenesis. Genetics 151, 1065–1079.

Zhang, P., Stankiewicz, R.L., 1998. Y-Linked male sterile mutations induced by P element in *Drosophila melanogaster*. Genetics 150, 735–744.

Zhang, Y.Q., Bailey, A.M., Matthies, H.J., Renden, R.B., Smith, M.A., Speese, S.D., Rubin, G.M., Broadie, K., 2001. *Drosophila* fragile X-related gene regulates the MAP1B homolog Futsch to control synaptic structure and function. Cell 107, 591–603.